



Micromotor-Based High-Yielding Fast Oxidative Detoxification of Chemical Threats**

Jahir Orozco, Guanzhi Cheng, Diana Vilela, Sirilak Sattayasamitsathit, Rafael Vazquez-Duhalt, Gabriela Valdés-Ramírez, On Shun Pak, Alberto Escarpa, Chengyou Kan, and Joseph Wang*

Rapid field conversion of chemical weapons into non-toxic products is one of the most challenging tasks in weapons of mass destruction (WMD) science.^[1] This is particularly the case for eliminating stockpiles of chemical warfare agents (CWAs) in remote storage field locations, where the use of large quantities of decontaminating reagents, long reaction times, and controlled mechanical agitation is impossible or undesired. New efficient “clean” technologies and (bio)-chemical processes are thus sought for detoxifying stored agents, counteracting nerve-agent attacks, and decommissioning chemical weapons. Environmentally friendly solutions of hydrogen peroxide, combined with suitable activators (e.g., bicarbonate), have been shown to be extremely useful for decontaminating a broad spectrum of CWAs to yield non-toxic products.^[2] These peroxide-based systems, which rely on the in situ generation of OOH^- nucleophiles, have recently replaced chlorine-based bleaching processes, which produce undesirable products, and have thus led to effective decontamination of the chemical agents GB (Sarin, isopropyl methylphosphonofluoridate), VX ((*S*)-[2-(diisopropylamino)ethyl] *O*-ethyl methylphosphonothioate), GD (Soman, pinacolyl methylphosphonofluoridate), and HD (sulfur mustard).^[2b] Yet, such an oxidative treatment commonly requires high peroxide concentrations (20–30%; approaching a stoichiometry of 1:50), along with prolonged operation and/or

mechanical agitation. Such reaction conditions are not suitable or not desired for eliminating stockpiles of CWAs in remote field settings or hostile storage locations, as large quantities of the reagents may not be transportable on military aircrafts and require special packaging and handling. The efficient elimination of chemical-weapon stockpiles in field locations thus remains a major challenge to the chemistry and defense communities.

Herein, we describe a powerful strategy that is based on self-propelled micromotors, for a high-yielding accelerated oxidative decontamination of chemical threats using low peroxide levels and no external agitation. Functionalized synthetic micromotors have recently demonstrated remarkable capabilities in terms of isolation and transport for diverse biomedical^[3] and environmental^[4] applications, but not in connection to increasing the yield and speed of chemical reactions. The new motor-based method relies on the use of peroxide-driven microtubular engines for the efficient self-mixing of a remediation solution, which dramatically accelerates the decontamination process. Fluid mixing is extremely important for enhancing the yield and speed of a wide range of chemical processes, including decontamination reactions, where quiescent conditions lead to low reaction efficiency and long operations. The observed mixing, which is induced by the peroxide-driven micromotor, is analogous to that reported for the motility of *E. coli* bacteria, where a large-scale collective motion has been shown to enhance diffusion processes.^[5a–c] Enhanced diffusion of passive tracers has also been observed in the presence of catalytic nanowire motors.^[6] Although the new micromotor strategy presented herein was applied to the accelerated, high-yielding, and simplified decontamination of organophosphate (OP) nerve agents, the concept could have broad implications for enhancing the efficiency and speed of a wide range of chemical processes in the absence of external agitation.

The concept of the micromotor/peroxide-based decontamination of chemical threats is illustrated in Figure 1. This new strategy relies on micromotors without mechanical stirring (Figure 1 A). A known number of micromotors were placed in a nerve-agent-contaminated solution, along with hydrogen peroxide (used as the oxidizing agent as well as the micromotor fuel), the peroxide activator (NaHCO_3 or NaOH), and the surfactant sodium cholate (NaCh), which was essential for bubble generation. The oxidative conversion of the OP nerve agent into *para*-nitrophenol (*p*-NP) was achieved under mild quiescent conditions that involve the in situ generation of OOH^- nucleophiles with no external stirring (Figure 1 B). The decrease in concentration of the OP

[*] Dr. J. Orozco,^[†] G. Cheng,^[†] D. Vilela,^[†] Dr. S. Sattayasamitsathit, Prof. R. Vazquez-Duhalt, Dr. G. Valdés-Ramírez, Dr. O. S. Pak, Prof. J. Wang
Departments of Nanoengineering and Mechanical Engineering
University of California San Diego
La Jolla, CA 92093 (USA)
E-mail: josephwang@ucsd.edu

G. Cheng,^[†] Prof. C. Kan
Tsinghua University, Beijing, 100084 (China)

D. Vilela,^[†] Prof. A. Escarpa
University of Alcalá
28871 Alcalá de Henares (Spain)

Prof. R. Vazquez-Duhalt
Center for Nanosciences and Nanotechnology, UNAM
Ensenada, 22800 (Mexico)

[†] These authors contributed equally to this work.

[**] This project received support from the Defense Threat Reduction Agency–Joint Science and Technology Office for Chemical and Biological Defense (HDTRA1-13-1-0002). G.C. and D.V. acknowledge financial support from the China Scholarship Council and the Spanish Science and Innovation Ministry, respectively. The authors thank Prof. M. Intaglietta and Dr. A. Tsai (UCSD) for the viscosity measurements.



Supporting information for this article is available on the WWW under <http://dx.doi.org/10.1002/anie.201308072>.

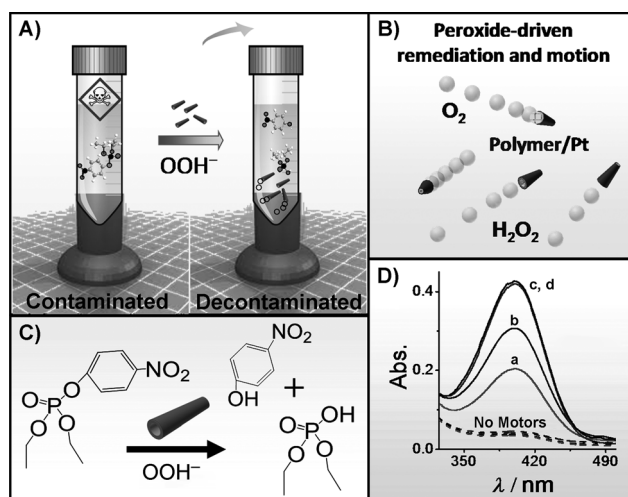


Figure 1. Micromotor-based accelerated oxidative detoxification of OP nerve agents. A, B) Placement of the micromotors in a contaminated aqueous solution, along with H_2O_2 as the oxidant/fuel and NaHCO_3 as the activator, leads to accelerated and high-yielding oxidative degradation because of an enhanced fluid motion that is induced by the movement of multiple microengines. C) The micromotor-based strategy allows rapid detoxification of chemical threats under mild conditions, and involves the in situ generation of OOH^- nucleophiles. D) The efficiency of the decontamination process was estimated spectrophotometrically by measuring the absorbance of the *p*-NP reaction product at 400 nm at different reaction times (a–d).

agent was monitored spectrophotometrically by measuring the absorbance of the *p*-NP product at 400 nm (Figure 1C).

The polymer-based microtubular engines were prepared by a template-based electrodeposition of a PEDOT/Pt bilayer^[7] (PEDOT = poly(3,4-ethylenedioxythiophene); for details, see the Supporting Information). The template fabrication process results in approximately 8 μm -long polymer/Pt microtubes that are efficiently propelled by the ejection of oxygen bubbles that are generated by the catalytic oxidation of hydrogen peroxide fuel at their inner Pt layer.^[3a,7] As will be discussed below, both the movement of the motors and their bubble generation contribute to the substantial fluid motion and to the accelerated decontamination process. Such motor-induced convection leads to a greatly enhanced remediation efficiency while using substantially lower peroxide concentrations, shorter reactions times, and no external stirring, compared to conventional peroxide detoxification methods.

To demonstrate the practical utility of the new micromotor-accelerated decontamination strategy, we examined the ability to decontaminate a variety of OP pesticides with analogous molecular structures, namely methyl paraoxon (MP), ethyl paraoxon (EP) and bis(4-nitrophenyl) phosphate (b-NPP). Figure 2 displays the absorbance signals of the *p*-NP

hydrolysis product of MP (—, Figure 2A), EP (—, Figure 2B) and NPP (—, Figure 2C) following a motor-accelerated oxidative reaction in a solution (15 mL) containing the OP compound (25 μM) and hydrogen peroxide (1.5%) for 20 min. These absorbance signals correspond to decomposition values of 96.1, 70.2, and 12.0% for MP, EP, and NPP, respectively. In contrast, negligible signals were obtained when the activated peroxide solution was reacted with these OP pesticides for the same duration, but without the micromotors (—, Figure 2A–C). Interestingly, negligible signals were also observed under similar conditions in the presence of the motors, but in the absence of the NaCh surfactant, which is thus essential for bubble development and motion (----, Figure 2A–C). Therefore, the Pt layer of the micromotors by itself does not enhance to the decontamination process. Overall, these results (Figure 2) demonstrate that micromotor movement is crucial for an efficient and rapid degradation process.

The efficiency of the new micromotor-based decontamination process depends on a variety of interdependent reaction variables. Knowledge of this interdependence can be helpful when optimizing the remediation process. For example, sample volume and remediation time displayed a strong interdependence effect on the decontamination efficiency (Figure 3; see also the Supporting Information, Figure S1A). The extent of decontamination was studied for

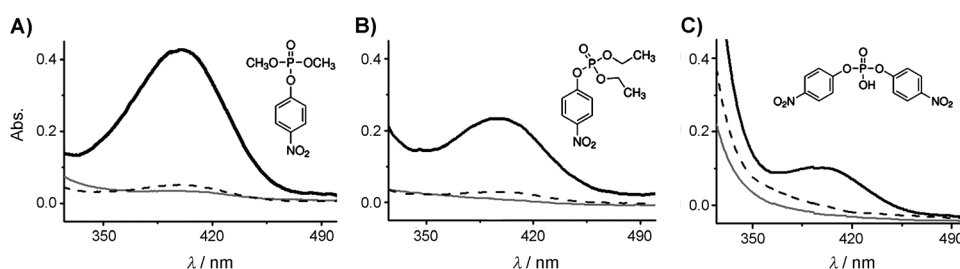


Figure 2. a) Absorbance spectra for the *p*-NP product obtained in the presence (—) and absence (---) of the micromotors, and with the motors not moving (----). Nerve-agent solutions (15 mL) containing MP (A), EP (B), and b-NPP (C) at a concentration of 25 μM , along with H_2O_2 (1.5%) and NaCh (2%; only for — and —), 0.1 M of the peroxide activator NaHCO_3 (A, B) or NaOH (C), and 5×10^5 micromotors (A–C). Reaction time: 20 min.

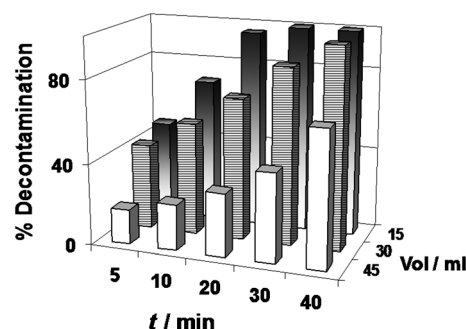


Figure 3. Effect of remediation time and sample volume on the decontamination efficiency. The efficiency was estimated from the absorbance signals of the *p*-NP product of MP (25 μM ; 5–40 min) for sample volumes of 15–45 mL. Reaction conditions: H_2O_2 (1.5%), NaCh (2%), NaHCO_3 (0.1 M), and 5×10^5 micromotors.

different volumes of an MP solution (15–45 mL) and for time periods ranging from 5–40 min. As expected, the extent of the decontamination increases to over 90% upon decreasing the sample volume and extending the reaction times. As will be illustrated below, an increase in the micromotor density can also be used for increasing the efficiency without extending the reaction time. Higher motor densities can also address the stoichiometric limitations, so that high reaction yields may still be achieved at elevated OP concentrations without increasing the amount of peroxide. The decontamination rates for three OP compounds in the presence (a–c) and absence (a'–c') of the micromotors are compared in Figure 4A. As expected for quiescent conditions, only negligible (<5%) decontamination of the nerve-agent solutions was

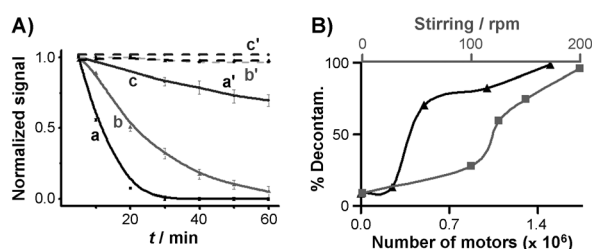


Figure 4. A) Time dependence of the oxidative decontamination of different nerve agents: MP (a, a'), EP (b, b'), and b-NPP (c, c') in the presence (a–c) and absence (a'–c') of micromotors. B) Effect of the number of motors (▲) and of the external magnetic stirring rate (■) on the decomposition of an aqueous MP solution; reaction time: 10 min. In the absence of motors (■), fluid convection is achieved by magnetic stirring. Reaction conditions: H_2O_2 (1.5%), NaCh (2%), NaHCO_3 (0.1 M) for MP and EP and NaOH (0.1 M) for b-NPP, and 5×10^5 micromotors.

observed over the entire period of 60 min (a'–c'). In contrast, the presence of the motors resulted in rapid hydrolysis of MP, EP, and b-NPP even within 20 min (96.1, 69.3, and 11.9% decontamination, respectively); after 40 min, decontamination efficiencies of 100, 97.7, and 20.9% were achieved (a–c). The differences in the detoxification efficiency of the three OP agents are consistent with the relative hydrolysis rate constants of these compounds.^[8] Whereas the decontamination of NPP was negligible when OOH^- that was generated from NaHCO_3 and H_2O_2 was used, higher degradation rates were observed when the OOH^- was obtained from NaOH and H_2O_2 .^[9] Even faster detoxification can be achieved by increasing the number of micromotors in the remediation solution. The influence of the number of micromotors is illustrated in Figure 4B (▲; see also Figure S2A) for a reaction time of 10 min. The efficiency of the MP hydrolysis increases from 70.5 to 82.1 and 98.6% upon increasing the number of micromotors from 5×10^5 to 1.0×10^6 and 1.5×10^6 , respectively.

To assess the fluid movement and the accelerated decontamination reaction that were induced by self-propelled micromotors, and to estimate the mixing capacity and the power input of the micromotors, the decontamination behavior (Figure 4B) was compared with that obtained in the

absence of the motors under well-defined forced convection conditions. For example, mixing the MP remediation solution with a magnetic stirrer at speeds of 100, 125, 150, and 200 rpm resulted in decontamination efficiencies of 20.5, 57.8, 71.4, and 95.2%, respectively (■, Figure 4B; see also Figure S2B(a–d)). Apparently, self-propulsion of approximately 1.5×10^6 micromotors in a quiescent solution leads to a very high detoxification efficiency (98.6%), which is slightly greater than that observed using the magnetic stirrer at 200 rpm (95.2%). Interpolating the magnetic stirring rate at which the same reaction efficiency is obtained as for the use of the micromotors allows an estimate of the mixing capacity and power consumption per unit mass of the fluid in a magnetically stirred flask at the interpolated rates, assuming a single rectangular paddle stirrer^[10] (for details, see the Supporting Information). The mixing capacities of quiescent solutions that contained different amounts of self-propelled micromotors were determined to be equivalent to stirring rates ranging from 99.2 to 208.5 rpm. Power (2.49×10^5 to 1.49×10^6) was thus found to be equivalent to a magnetic consumption per unit fluid mass that ranged from 1.3 to $10.8 \text{ cm}^2 \text{ s}^{-3}$, depending on the number of motors involved. By dividing the equivalent power consumption in the magnetically stirred flask by the number of micromotors, an average power per micromotor of $(11.0 \pm 2.1) \text{ pW}$ is obtained. The accelerated decontamination achieved by the motor-induced self-stirring of the remediation solution can be attributed to the large-scale collective motion of the micromotors, as hydrodynamic interactions lead to an enhanced mixing. Similar dynamics of self-organization and enhanced diffusion rates were observed in the presence of swimming bacteria^[5] and nanowire motors.^[6] Collective motion in active suspensions was also reported in theoretical studies.^[11] The continuous bubble generation by microtubular engines is also expected to contribute to the solution mixing and to have profound effects on the accelerated decontamination. Microbubbles have previously been used to enhance mixing in microfluidic systems,^[12] and their exact role in these accelerated chemical reactions will be characterized in future studies.

The chemical structure of the OP compound has a profound effect upon the efficiency of the decontamination process (Figure 4A). We also applied the motor-based detoxification approach to organothiophosphate nerve agents, which contain a P=S instead of a P=O bond. Only a low yield of decontamination was observed for P=S containing methyl parathion, with only a slight increase in the absorbance signal of the reaction product (Figure S3). Such behavior is in agreement with structure–reactivity correlations for the hydrolysis of OP compounds.^[8] The lower conversion that was observed for parathion compared with its oxo analogue (paraoxon), is attributed to the fact that phosphorothioates are less reactive and more stable against hydrolytic degradation than the corresponding oxo (P=O) derivatives. The more pronounced polarization of the P=O bond, which is due to the higher electronegativity of the oxygen atom, compared to the P=S bond results in a more electropositive phosphorus atom, which facilitates nucleophilic attack on the phosphorus atom.^[8]

In conclusion, we have demonstrated a new strategy for the oxidative detoxification of OP nerve agents that is based on self-propelled micromotors. The repeated movement of multiple motors across a peroxide-activated contaminated sample results in greatly enhanced mass transport (without external agitation), and hence leads to a higher decontamination efficiency while using significantly shorter reaction times and lower peroxide concentrations compared to common CWA neutralization processes. The new micromotor strategy is expected to enhance the efficiency and speed of decontamination reactions of a broad range of threats and pollutants, but also of chemical processes in general. Implementation of the new motor-based detoxification strategy for the decomposition of a broad range of CWAs requires tailoring of the reaction conditions for each specific threat. Efforts in this direction, and towards understanding the exact impact of the motor movement upon the overall reaction yields, are currently being pursued in our laboratories.

Received: September 14, 2013

Published online: October 24, 2013

Keywords: chemical weapons · detoxification · nanomachines · oxidation · phosphorus

- [1] a) Y.-C. Yang, J. A. Baker, J. A. Ward, *Chem. Rev.* **1992**, 92, 1729; b) B. M. Smith, *Chem. Soc. Rev.* **2008**, 37, 470; c) K. Kim, O. G. Tsay, D. A. Atwood, *Chem. Rev.* **2011**, 111, 5345.
- [2] a) G. Wagner, Y. C. Yang, *Ind. Eng. Chem. Res.* **2002**, 41, 1925; b) G. Wagner, L. Porcell, D. Sorrick, G. Lawson, C. Wells, C. Reynolds, D. Ringelberg, K. Foley, G. Lumetta, D. Blanchard, *Ind. Eng. Chem. Res.* **2010**, 49, 3099.
- [3] a) J. Wang, *Nanomachines: Fundamentals and Applications*, Wiley-VCH, Weinheim, **2013**; b) J. Wang, *Lab Chip* **2012**, 12, 1944.
- [4] a) M. Guix, J. Orozco, M. García, W. Gao, S. Sattayasamitsathit, A. Merkoci, A. Escarpa, J. Wang, *ACS Nano* **2012**, 6, 4445; b) J. Orozco, V. García-Gradilla, M. D'Agostino, W. Gao, A. Cortés, J. Wang, *ACS Nano* **2013**, 7, 818.
- [5] a) X. Wu, A. Libchaber, *Phys. Rev. Lett.* **2000**, 84, 3017; b) M. Kim, K. Breuer, *Phys. Fluids* **2004**, 16, L78; c) A. Sokolov, R. Goldstein, F. Feldchtein, I. Aranson, *Phys. Rev. E* **2009**, 80, 0310903.
- [6] G. Miño, T. E. Mallouk, T. Darnige, M. Hoyos, J. Dauchet, R. Soto, Y. Wang, A. Rousselet, E. Clement, *Phys. Rev. Lett.* **2011**, 106, 048102.
- [7] W. Gao, S. Sattayasamitsathit, A. Uygun, A. Pei, A. Ponedal, J. Wang, *Nanoscale* **2012**, 4, 2447.
- [8] a) S. B. Hons, F. M. Raushel, *Biochemistry* **1999**, 38, 1159; b) T. R. Fukuto, *Environ. Health Perspect.* **1990**, 87, 245.
- [9] J. Domingos, E. Longhinotti, T. Brandao, L. Santos, M. Eberlin, C. Bunton, F. Nome, *J. Org. Chem.* **2004**, 69, 7898.
- [10] S. Nagata, *Mixing: Principles and Applications*, Wiley, New York, **1975**, pp. 24–38.
- [11] a) D. Saintillan, M. Shelley, *Phys. Rev. Lett.* **2007**, 64, 011902; b) R. Simha, S. Ramaswamy, *Phys. Rev. Lett.* **2002**, 89, 058101; c) J. Hernandez-Ortiz, C. Stoltz, M. Graham, *Phys. Rev. Lett.* **2005**, 95, 204501; d) H. Grégoire, Y. Chaté, Y. Tu, *Phys. Rev. E* **2001**, 64, 011902.
- [12] P. Garstecki, M. A. Fischbach, G. M. Whitesides, *Appl. Phys. Lett.* **2005**, 86, 244108.